

The public reporting burden for this collection of information is estimated to average 1 hour per response, including the time for reviewing instructions, searching existing data sources, gathering and maintaining the data needed, and completing and reviewing the collection of information. Send comments regarding this burden estimate or any other aspect of this collection of information, including suggestions for reducing this burden, to Washington Headquarters Services, Directorate for Information Operations and Reports, 1215 Jefferson Davis Highway, Suite 1204, Arlington VA, 22202-4302. Respondents should be aware that notwithstanding any other provision of law, no person shall be subject to any penalty for failing to comply with a collection of information if it does not display a currently valid OMB control number.
PLEASE DO NOT RETURN YOUR FORM TO THE ABOVE ADDRESS.

1. REPORT DATE (DD-MM-YYYY) 17-11-2017	2. REPORT TYPE Final Report	3. DATES COVERED (From - To) 15-Apr-2014 - 14-Apr-2017
---	--------------------------------	---

4. TITLE AND SUBTITLE Final Report: Targeting and Triggering using Liquid Crystals: Reactive Chemical Systems	5a. CONTRACT NUMBER W911NF-14-1-0140
	5b. GRANT NUMBER
	5c. PROGRAM ELEMENT NUMBER 611102

6. AUTHORS	5d. PROJECT NUMBER
	5e. TASK NUMBER
	5f. WORK UNIT NUMBER

7. PERFORMING ORGANIZATION NAMES AND ADDRESSES University of Wisconsin - Madison The Board of Regents of the University of Wisconsin S Suite 6401 Madison, WI 53715 -1218	8. PERFORMING ORGANIZATION REPORT NUMBER 1.00
---	--

9. SPONSORING/MONITORING AGENCY NAME(S) AND ADDRESS (ES) U.S. Army Research Office P.O. Box 12211 Research Triangle Park, NC 27709-2211	10. SPONSOR/MONITOR'S ACRONYM(S) ARO
	11. SPONSOR/MONITOR'S REPORT NUMBER(S) 65331-CH.21

12. DISTRIBUTION AVAILABILITY STATEMENT Approved for public release; distribution is unlimited.
--

13. SUPPLEMENTARY NOTES The views, opinions and/or findings contained in this report are those of the author(s) and should not be construed as an official Department of the Army position, policy or decision, unless so designated by other documentation.

14. ABSTRACT

15. SUBJECT TERMS

16. SECURITY CLASSIFICATION OF:			17. LIMITATION OF ABSTRACT UU	15. NUMBER OF PAGES	19a. NAME OF RESPONSIBLE PERSON NICHOLAS ABBOTT
a. REPORT UU	b. ABSTRACT UU	c. THIS PAGE UU			19b. TELEPHONE NUMBER 608-265-5278

RPPR Final Report

as of 19-Apr-2018

Agency Code:

Proposal Number: 65331CH

Agreement Number: W911NF-14-1-0140

INVESTIGATOR(S):

Name: PhD NICHOLAS L ABBOTT abbott@eng

Email: NLABBOTT@WISC.EDU

Phone Number: 6082655278

Principal: Y

Organization: **University of Wisconsin - Madison**

Address: The Board of Regents of the University of Wisconsin Sys, Madison, WI 537151218

Country: USA

DUNS Number: 161202122

EIN: 396006492

Report Date: 14-Jul-2017

Date Received: 17-Nov-2017

Final Report for Period Beginning 15-Apr-2014 and Ending 14-Apr-2017

Title: Targeting and Triggering using Liquid Crystals: Reactive Chemical Systems

Begin Performance Period: 15-Apr-2014

End Performance Period: 14-Apr-2017

Report Term: 0-Other

Submitted By: PhD NICHOLAS ABBOTT

Email: NLABBOTT@WISC.EDU

Phone: (608) 265-5278

Distribution Statement: 1-Approved for public release; distribution is unlimited.

STEM Degrees: 3

STEM Participants: 4

Major Goals: Supramolecular assemblies offer exciting opportunities for amplification of targeted molecular-level transformations into functional outcomes (e.g., release of an agent or a change in a mechanical or optical property). The major goal of this project is to use thermotropic liquid crystals as an important and representative class of supramolecular assemblies to develop general principles by which targeted interfacial molecular events can trigger changes in molecular organization on optical scales. The approach builds from recent observations by the PI that ionic phenomena, including specific ion effects, and the chirality of biological adsorbates can influence the internal configurations of micrometer-sized liquid crystalline droplets that are dispersed in water. These observations suggest a variety of unexplored mechanisms by which the presence and transformation of adsorbates at the interfaces of liquid crystals can trigger changes in ordering that are easily transduced at the micrometer scale. The proposal is organized into two parts. First, a series of fundamental physicochemical investigations will be conducted to elucidate the basic mechanisms by which ion concentration, ion type and adsorbate chirality impact interfacial phenomena involving micrometer-sized droplets of liquid crystals. Second, these mechanisms of triggering liquid crystalline droplets will be explored in the context of droplets decorated with amphiphiles, polyelectrolytes and oligopeptides. This second thrust includes studies of amphiphilic block copolymers designed with mesogenic and oligopeptide side-chains that can be processed by enzymes to explore translation of the fundamental physicochemical phenomena described in the first part of the proposal into initial designs of multifunctional amphiphiles for targeting and triggering using liquid crystals. In the long term, the knowledge emerging from this research will enable new strategies for (i) amplification of molecular events into the optical scale, (ii) stabilization of emulsions, (iii) design of stimuli-responsive materials, (iv) and interfacial designs of chemical and biological sensors.

Accomplishments: Please see upload section

Training Opportunities: The project has provided outstanding opportunities for undergraduate and graduate students to participate in research in colloid and interface science, including interdisciplinary collaboration with researchers at UC San Diego.

Results Dissemination: The results of this research were published in 19 peer-reviewed manuscripts (all acknowledging support of this grant). In addition, the PI gave oral presentations at a range of conferences, including national meetings of the ACS, APS and MRS. In addition, the PI gave more the 20 seminars at universities on his research.

RPPR Final Report as of 19-Apr-2018

Honors and Awards: 2017 6th Somer Lectures, Middle East Technical University, Ankara, Turkey.
2017 Paul J. Berics Professorship, University of Wisconsin
2016 42nd Annual Harry G. Fair Memorial Lecture, University of Oklahoma
2016 The William H. Schwartz Lecture, The Johns Hopkins University
2016 Elected Fellow of the American Physical Society
2016 American Chemical Society Award in Colloid and Surface Chemistry
2016 Elected to American Institute of Biological and Medical Engineers
2016 42nd Annual Harry G. Fair Memorial Lecture, University of Oklahoma
2015 Byron Bird Award
2015 Founders Lecturer, University of California, Los Angeles
2014 Hilldale Professorship
2014 Elected Member of National Academy of Engineering

Protocol Activity Status:

Technology Transfer: Nicholas Abbott is a co-founder of both Platypus Technologies LLC and Imbed Biosciences Inc, each of Madison WI, which are focused on the translation of advances in the design of functional materials interfaces into (I) analytic technologies (Platypus) and (II) new approaches to accelerated wound healing (Imbed Biosciences). Understanding the design of soft material interfaces is critical to the technologies being developed by both companies, and several approaches being explored within the current grant have the potential to impact these companies. In 2016, Imbed Biosciences received FDA approval for a new wound dressing that accelerates healing of chronic wounds.

Nicholas Abbott also gave a seminar at Edgewood ECBC in 2016, in which he described advances in the design of responsive liquid crystal interfaces to DoD scientists and engineers.

PARTICIPANTS:

Participant Type: PD/PI

Participant: Nicholas Lawrence Abbott

Person Months Worked: 1.00

Funding Support:

Project Contribution:

International Collaboration:

International Travel:

National Academy Member: Y

Other Collaborators:

Participant Type: Graduate Student (research assistant)

Participant: Yu Yang

Person Months Worked: 6.00

Funding Support:

Project Contribution:

International Collaboration:

International Travel:

National Academy Member: N

Other Collaborators:

Participant Type: Graduate Student (research assistant)

Participant: Travis Nelson

Person Months Worked: 6.00

Funding Support:

Project Contribution:

International Collaboration:

International Travel:

National Academy Member: N

Other Collaborators:

Participant Type: Postdoctoral (scholar, fellow or other postdoctoral position)

RPPR Final Report
as of 19-Apr-2018

Participant: Joel Pendery

Person Months Worked: 4.00

Funding Support:

Project Contribution:

International Collaboration:

International Travel:

National Academy Member: N

Other Collaborators:

Participant Type: Graduate Student (research assistant)

Participant: Peter Mushenheim

Person Months Worked: 6.00

Funding Support:

Project Contribution:

International Collaboration:

International Travel:

National Academy Member: N

Other Collaborators:

ARTICLES:

Publication Type: Journal Article

Peer Reviewed: Y

Publication Status: 1-Published

Journal: Langmuir

Publication Identifier Type: DOI

Publication Identifier: 10.1021/la500978s

Volume: 0

Issue: 0

First Page #: 0

Date Submitted:

Date Published:

Publication Location:

Article Title: Helical versus All-Trans Conformations of Oligo(ethylene glycol)-Terminated Alkanethiol Self-Assembled Monolayers

Authors:

Keywords: oligoethylene glycol, conformations, x-ray absorption spectroscopy, monolayers

Abstract: The complex mixture of conformational states exhibited by oligo(ethylene glycol)-terminated alkanethiols on Ag and Au surfaces is explored by polarization-dependent X-ray absorption spectroscopy. Three self-assembled monolayers (SAMs) with known helical or all-trans conformations are used as references to characterize a SAM with unknown conformations. This case study is used as a prototype for developing a systematic framework to extract the conformations of SAMs from the polarization dependence of several orbitals. In the case at hand, these are associated with the C₁H/Rydberg bonds of the alkane, the C₁H/Rydberg bonds of ethylene glycol, and the C₁C bonds of the backbone. The C₁H/Rydberg orbitals of the alkane and ethylene glycol are distinguished via the chemical shift of the corresponding C 1s core levels.

Distribution Statement: 1-Approved for public release; distribution is unlimited.

Acknowledged Federal Support:

RPPR Final Report as of 19-Apr-2018

Publication Type: Journal Article Peer Reviewed: Y **Publication Status:** 1-Published

Journal: Angewandte Chemie International Edition

Publication Identifier Type: DOI

Publication Identifier: 10.1002/anie.201402770

Volume: 53

Issue: 31

First Page #: 8079

Date Submitted:

Date Published:

Publication Location:

Article Title: Liquid Crystals Anchored on Mixed Monolayers of Chiral versus Achiral Molecules: Continuous Change in Orientation as a Function of Enantiomeric Excess

Authors:

Keywords: chirality, monolayers, liquid crystals, anchoring

Abstract: The orientations of liquid crystals (LCs) anchored on monolayers formed from mixtures of chiral versus achiral molecules were compared. Changes in the enantiomeric excess of mixed monolayers of chiral dipeptides gave rise to continuous changes in the orientations of nematic LCs, allowing arbitrary tuning of the azimuthal orientations of LCs over a range of 100 degrees. In contrast, the same LCs exhibited discontinuous changes in orientation on surfaces presenting mixtures of achiral molecules. These striking differences in the anchoring of LCs on surfaces presenting chiral versus achiral molecules provide insights into the molecular origins of ordering transitions of LCs, and provide new principles based on chiral monolayers for the rational design of surfaces that permit continuous tuning of the orientations of LCs.

Distribution Statement: 1-Approved for public release; distribution is unlimited.

Acknowledged Federal Support:

Publication Type: Journal Article Peer Reviewed: Y **Publication Status:** 1-Published

Journal: Langmuir

Publication Identifier Type: DOI

Publication Identifier: 10.1021/la501596b

Volume: 0

Issue: 0

First Page #: 0

Date Submitted:

Date Published:

Publication Location:

Article Title: Surfactant-Induced Ordering and Wetting Transitions of Droplets of Thermotropic Liquid Crystals "Caged" Inside Partially Filled Polymeric Capsules

Authors:

Keywords: liquid crystals, microdroplets, anchoring transitions, interfaces, ordering, polymeric capsules

Abstract: We report a study of the wetting and ordering of thermotropic liquid crystal (LC) droplets that are trapped (or "caged") within micrometer-sized cationic polymeric microcapsules dispersed in aqueous solutions of surfactants. When initially dispersed in water, we observed caged, near-spherical droplets of E7, a nematic LC mixture, to occupy ~40% of the interior volume of the polymeric capsules [diam. = $6.7 \pm 0.3 \mu\text{m}$; formed via covalent layer-by-layer assembly of branched polyethyleneimine and poly(2-vinyl-4,4-dimethylazlactone)] and to contact the interior surface of the capsule wall at an angle of $\sim 157 \pm 11^\circ$. The internal ordering of LC within the droplets corresponded to the so-called bipolar configuration (distorted by contact with the capsule walls). While the effects of dodecyltrimethylammonium bromide (DTAB) and sodium dodecylsulfate (SDS) on the internal ordering of "free" LC droplets are similar, we observed the two surfactants to trigger strikingly different wetting and configur

Distribution Statement: 1-Approved for public release; distribution is unlimited.

Acknowledged Federal Support:

This grant has focused on using thermotropic liquid crystals to develop general principles by which targeted interfacial molecular events trigger changes in supramolecular organization on optical scales. Progress has occurred in three broad areas. First, a series of fundamental physicochemical investigations have been initiated to elucidate the basic mechanisms by which macroions (polyelectrolytes) and adsorbate chirality impact ordering of micrometer-sized droplets of liquid crystals. Second, we investigated the effects of chiral adsorbates and adsorbates on liquid crystalline systems, including the influence of chirality on colloidal self-assembly processes at the interfaces of liquid crystals. Third, the above-described mechanisms of triggering liquid crystals were explored in the context of droplets decorated with amphiphilic block copolymers designed with mesogenic and oligopeptide side-chains that can be processed by enzymes. Finally, we explored how the partitioning of amphiphiles can trigger changes in the ordering of liquid crystals.

Influence of ionic adsorbates (monomeric and polymeric) on the orientational ordering of liquid crystals at aqueous interfaces

Liquid crystals are stimuli-responsive materials and a key goal of our research was to develop an understanding of the types of interfacial interactions that trigger their ordering transitions at aqueous interfaces. We focused on exploring the role of ions and interfacial charge on the ordering of LC droplets. Specifically, we performed a number of experiments to explore parameters that we predicted would influence the charging of LC droplets and thus impact the contribution of electrical double layers to the anchoring of the LC. Specifically, we investigated

- i. Three LCs that differ in their dielectric properties (5CB, TL205, or MLC2080)
- ii. Bare LC droplets, or LCs coated with polyelectrolyte (PAH, PDADMAC, or PSS)
- iii. Aqueous electrolyte concentrations (0 mM - 1 M)
- iv. pH (neutral to 12.5)

In addition, we developed a simple model of the formation of electrical double layers within the spherical geometry of LC droplets and calculated the effects of double layers on anchoring energies. Of particular relevance is the effect of the LC droplet size on the anchoring energy of the LC. Specifically, as shown in Figure 1, we predicted that the overlap of the electrical double layer will decrease the electrostatic contribution to the anchoring energy of the LC. This identifies a mechanism by which the ordering of the LC is size-dependent, an observation that was confirmed in experiments. Figure 1 shows anchoring energies calculated using $T = 298$ K, zeta potential of -60 mV, and the

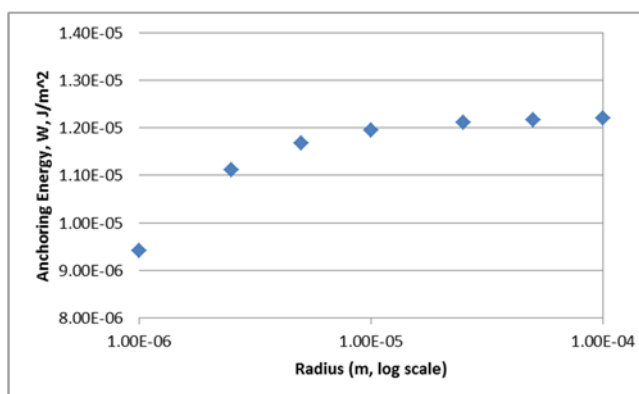


Figure 1: Change in anchoring energy of nematic 5CB droplets calculated as a function of the LC droplet radius

aqueous NaCl concentration of 1M as a function of the LC droplet size.

To test predictions such as those shown above, we performed measurements in which we quantified the ordering of LCs within microdroplets as (i) a function of the salt concentration and (ii) as a function of the polyelectrolyte adsorbed to the surfaces of the droplets. Figure 2 below shows results obtained with 2-4 micrometer-sized droplets of 5CB onto which we adsorbed the polyelectrolytes PAH, PDADMAC or PSS. Inspection of Figure 2 reveals that both the identity of the adsorbed polyelectrolytes and the NaCl concentration impacts the ordering of the LC. Interestingly, cationic polymers promote preradial or radial configurations of the LC droplets, with the effects being dependent on the electrolyte concentration. We also observed the ordering of the LC droplets to depend on the size of the droplets.

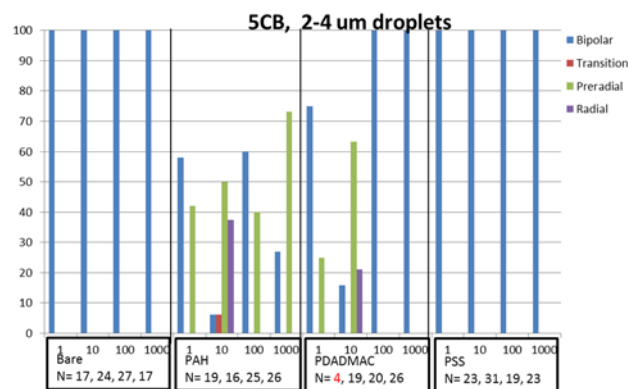


Figure 2: Ordering of nematic 5CB droplets in the presence of polyelectrolytes (PAH, PDADMAC and PSS), and as a function of added NaCl concentration.

Influence of chiral adsorbates/absorbates on the orientational ordering of liquid crystals

A second focus of the grant was directed to an investigation of how chiral adsorbates influence the ordering of LC droplets. While a number of theoretical predictions exist regarding the configurations of chiral LC droplets, very few experimental tests of the predictions have been reported. To this end, chiral nematic 5CB droplets were prepared by homogenizing 4 μL 5CB containing 1 % wt/wt of chiral dopant S-811 in 2 mL water for 30 seconds. Figure 3A-D show representative bright field and polarized light micrographs of a chiral nematic LC droplet adopting a so-called radial spherical structure (RSS), which was most commonly observed in our experiments. Inspection of Figure 3 reveals a double helix of two cholesteric disclination lines that emerges along a direction from the center of the droplet to the surface (evidence from side view of the droplet, Figure 3 A and B). This configuration is consistent with the simulations results

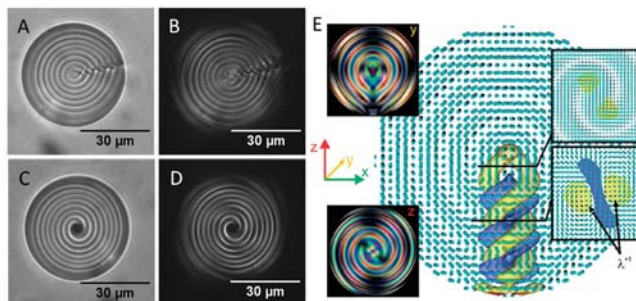


Figure 3. Representative bright field (A and C) and polarized light micrographs (B and D), and simulated director field (E) of a chiral nematic LC droplet adopting radial spherical structure (RSS). (A-D) was captured from one droplet viewed along (A and B) y, and (C and D) z axes. The insets in (E) show the director at marked cross sections and simulated polarization micrographs viewed along y and z axes. (E) was adapted from predictions by Zumer et al from Slovenia.

by Zumer et al from Slovenia. (Figure 3E). We also observed a range of other chiral LC droplet configurations, the frequency of which depend on the size of the LC droplets.

We also investigated the behaviors of colloids at the surfaces of nematic LC droplets dispersed in aqueous phases. When the nematic droplets exhibited a so-called bipolar configuration (with two topological defects [surface point defects] at the opposite poles), we measured 1 μm -in-diameter colloids adsorbed at the interfaces of the LC droplets to position themselves at one of the two poles. The localization of the colloids was determined to arise from the high elastic free energy density in the vicinity of the poles. When multiple colloids adsorbed at the aqueous interfaces of the nematic droplets, we observed the colloids to concentrate at the poles and form hexagonal assemblies under the influence of LC-mediated elastic interactions (the charged colloids also exhibited electrostatic repulsions). We moved also beyond achiral nematic LCs to explore LCs with distinct ordering symmetries (specifically, chirality) as the basis of an expanded palette of templates for positioning colloids. Specifically, we have revealed that cholesteric LCs, which are characterized by a helical twist orthogonal to the director of the LC, direct the formation of colloidal arrangements (such as precisely spaced colloidal pairs) that cannot be accessed through use of achiral nematic LCs or isotropic liquids.

Specifically, we investigated the internal configurations of aqueous dispersions of droplets of cholesteric liquid crystals (LCs; 5-50 μm -in-diameter; comprised of 4-cyano-4'-pentylbiphenyl and 4-(1-methylheptyloxycarbonyl)phenyl-4-hexyloxybenzoate) and their influence on the positioning of surface-adsorbed colloids (0.2 or 1 μm -in-diameter polystyrene (PS)). When $N = 2D/P$ was less than 4, where D is the droplet diameter and P is the cholesteric pitch, the droplets adopted a twisted bipolar structure (TBS) and colloids were observed to assume positions at either the poles or equator of the droplets. A statistical analysis of the distribution of locations of the colloids revealed a potential well of depth 2.7 kBT near the equator. In contrast, for $N > 4$, a majority of the droplets exhibited a radial spherical structure (RSS) characterized by a pair of closely spaced surface defects (angle of separation with respect to the center of the droplet $\theta < 5^\circ$) connected by a disclination winding to/from the droplet center, which led to the positioning of pairs of colloids with well-defined spacing at these surface defects. The separation of the pairs of surface-adsorbed colloids was colloid size-dependent, ranging from $1.11 \pm 0.04 \mu\text{m}$ for 1 μm -in-diameter

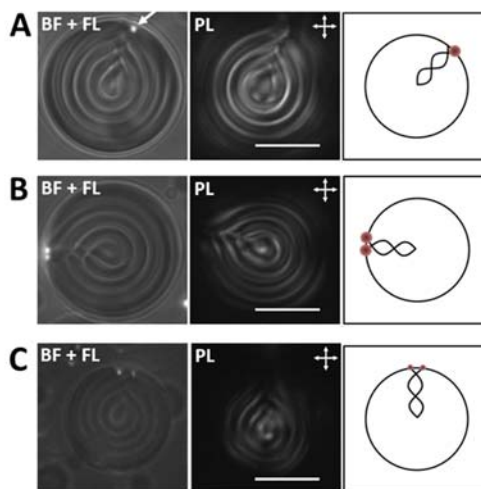


Fig. 4. Colloids positioned on RSS droplets. Bright field, polarized light micrographs and corresponding sketches showing (A) one 1 μm -in-diameter PS colloid, (B) two 1 μm -in-diameter PS colloids, and (C) two 200 nm-in-diameter PS colloids localized at surface point defects. Droplets of 2.5 wt % S-811/5CB dispersed in water. Scale bars: 10 μm .

colloids to $1.7 \pm 0.2 \mu\text{m}$ for 200 nm-in-diameter colloids. We also observed long-lived metastable configurations in which the two surface point defects were separated by much larger distances (corresponding to populations with angles of $\theta = 20 \pm 10^\circ$ and $85 \pm 10^\circ$ with respect to the center), and observed these pairs of defects to also position pairs of colloids (Figure 4). A third configuration, the diametrical spherical structure (DSS) was also observed. We found experimentally that the DSS is composed of disconnected defect rings positioned along the diameter of the droplet. Overall, these results reveal that the rich palette of defects exhibited by confined cholesteric LC systems (equilibrium and metastable) provide the basis of a versatile class of templates that enable the surface positioning of colloids in ways that are not possible with achiral LC droplets. Such responses of microparticles to changes in the configurations of LC droplets suggest a range of possible approaches whereby microparticles can be used in strategies for targeting and triggering.

An additional thrust of our work involving chiral nematic phases address systems containing high concentrations of chiral dopants. At high loadings of chiral dopant in a nematic LC, well-defined three dimensional networks of double twisted cylinders are known to form. These are described as blue phases. Between the double twisted cylinders, periodic arrays of defects appear (Fig. 5A and B). These periodic arrays of defects underlie many properties of BPs, including their optical appearance due to Bragg diffraction. To date, the majority of studies of BPs have been carried out in bulk systems. Our efforts went beyond past studies by investigating the effects of confinement on the structure and stability of BPs. Specifically, we have conducted an experimental

study of BPs confined to spherical droplets. Our results indicate that, in addition to the so-called BP I and II, several new morphologies arise under confinement, whose complexity increases with the chirality of the medium. They also

suggest that confinement increases the range of stability of BP, thereby providing intriguing prospects for use of these systems as stimuli-responsive supramolecular materials.

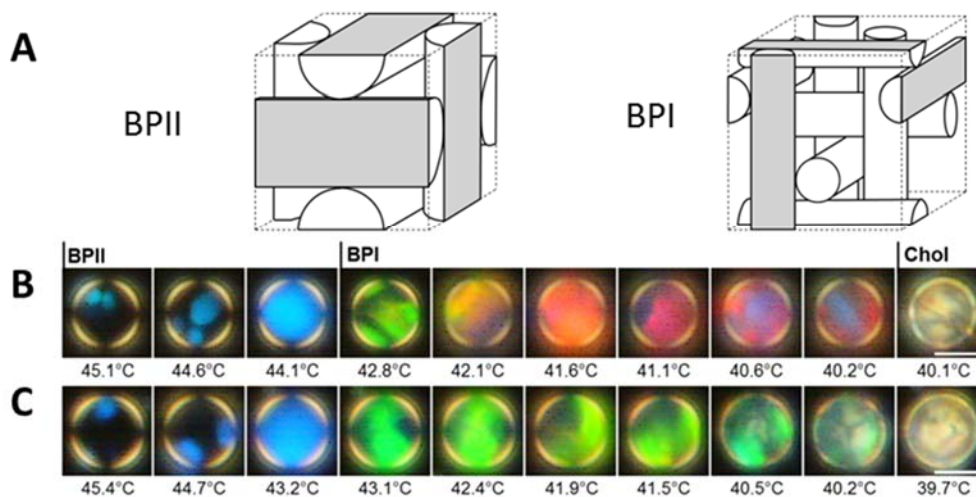


Figure 5. (A) Organization of double-twist cylinders in BPI and BPII. Optical micrographs (cross-polars, reflection mode) of droplets of 35 wt% S-811 doped MLC 2142 incubated in (B) water, and (C) 0.1 mM DLPC in water at the indicated temperatures. Samples were cooled from 50.0°C at 0.5°C/min. Scale bars: 10 μm .

Specifically, we investigated BP droplets dispersed in water, and have made a number of interesting observations regarding how temperature and adsorbates impact the stability of the BPs. These experiments revealed that below a size of about $\sim 4\mu\text{m}$, the Iso-BPII transition temperatures are lowered but BPII-BPI and BPI-Chol transition temperatures do not change substantially. For example, we observed Iso-BPII transition temperature of $\sim 2\mu\text{m}$ -in-diameter droplets at $43.9\text{ }^\circ\text{C}$, whereas at size of $\sim 4\mu\text{m}$ and larger droplets such transition occurred at $\sim 45.0\text{ }^\circ\text{C}$. This is a significant drop compared to overall $3\text{-}4\text{ }^\circ\text{C}$ stability region of BPs.

In addition, we have investigated the influence of interfacial adsorbates on the thermal stability of the BP droplets. Interestingly, BP droplets incubated with and without the presence of DLPC (1,2-dilauroyl-*sn*-glycero-3-phosphocholine) in water exhibit distinct optical responses. Figure 5B-C shows two $\sim 14\mu\text{m}$ -in-diameter droplets. Although the presence of DLPC did not affect the transition temperatures significantly, the optical appearance (caused by Bragg diffraction from the lattice of defects and thus influenced by the size and orientation of the BP unit cells with respect to the observer) was changed. Specifically, the optical appearance of the “naked” BPI droplets was temperature dependent (the color changed from green to red during cooling) whereas the droplets incubated in 0.1 mM DLPC did not exhibit this change. We have observed such effects at DLPC concentrations as low as $1\mu\text{M}$. This interesting observation suggests a preferential alignment and stabilization of the size of the unit cell of the BP with respect to the surface of the droplets.

Design of Responsive Peptide-Polymer Amphiphiles

As part of collaborative research with Professor Nathan Gianneschi from University of California-San Diego over the period of the grant, we leveraged our above-described observations of the effect of interfacial adsorbates on orientations of LCs to explore designs of biologically active peptide-polymer amphiphiles (PPA) for mediating enzymatically triggered optical responses in thermotropic liquid crystal (LC) microdroplets. The PPAs were designed and synthesized by the Gianneschi group to possess biphenyl side-chains to promote assembly at LC microdroplet interfaces and with peptidic moieties for enzymatic processing. We showed that enzymatic cleavage of the PPAs triggered changes in PPA-surfactant complexes formed at the interface of the LC, thus giving rise to an easily observable optical response to the enzymatic reaction. The combined use of PPAs

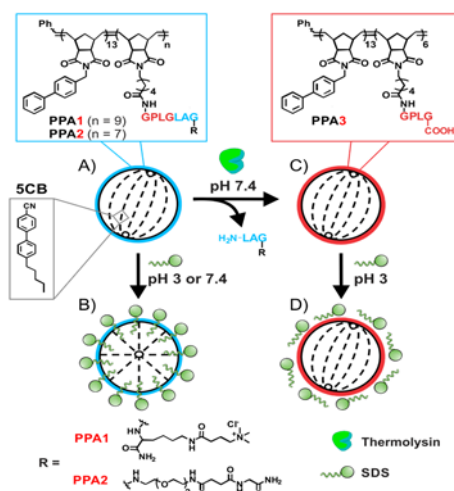


Figure 6. PPA-programmed LC microdroplet response to enzymatic reactions at their aqueous interface. (A) PPA-laden 5CB droplet in bipolar configuration. (B) PPA-laden 5CB droplet in radial configuration after exposure to SDS at either pH 3 or pH 7.4. (C) PPA-laden 5CB droplet in bipolar configuration after *in situ* enzyme treatment at pH 7.4. (D) Enzyme processed PPA-laden 5CB droplet in bipolar configuration after exposure to SDS at pH 3.

and surfactants represents a simple and modular strategy for targeting and triggering biomolecular events at LC microdroplet interfaces. PPAs were synthesized via ring-opening metathesis polymerization (ROMP) using norbornene-based monomers containing either biphenyl moieties or peptidic moieties (GPLGLAGK for PPA1, GPLGLAG for PPA2) to form hydrophobic and hydrophilic blocks, respectively (resulting ring-opened products as polymers are shown in Figure 6). The biphenyl group was used as the hydrophobic block to promote the co-assembly of the PPA at the interface of the biphenyl-based LC. The amino acid sequence of the peptidic moieties incorporated into the PPAs was selected to be enzymatically processable by thermolysin. We prepared PPA3 to serve as a mimic, or analogue of the enzymatic product of PPA1 and 2 (Figure 6).

Prior to assembly of PPAs at the interface of LCs and to our exploration of the influence of PPA-surfactant complexes on LC ordering, we characterized the surface activity of the PPAs by measuring their surface pressure-area (Π -A) isotherms at the aqueous/air interface at physiological pH 7.4 (Figure 7). Inspection of Figure 7A reveals that PPAs form stable monolayers at the surface of PBS solutions and that the Π -A isotherms are dependent on the structure of the PPAs. By rescaling the Π -A isotherms to the interfacial concentration of peptidic moieties presented by each PPA, we found that PPA1 and PPA2 were similar to each other but significantly different from PPA3 (Figure 7B). This result indicates that the peptidic moieties of PPA1 and PPA2 play a central role in determining the interfacial properties of the PPAs. Therefore, from these results we concluded that enzymatic cleavage of the peptide side-chain, which generates structures analogous to PPA3, would lead to substantial changes in interfacial properties. In addition, we note that PPA3 differs from PPA1 and PPA2 by the presence of a C-terminal carboxylic acid (Figure 6). Consistent with this difference in chemical functionality, we predicted that the Π -A isotherms of PPA3 but not PPA1 nor PPA2 would change with acidification of the PBS (Figure 7). The pH-dependent change in the Π -A isotherm of PPA3 likely originates from protonation of carboxylate groups and reduction in the electrostatic contribution to the surface pressure.

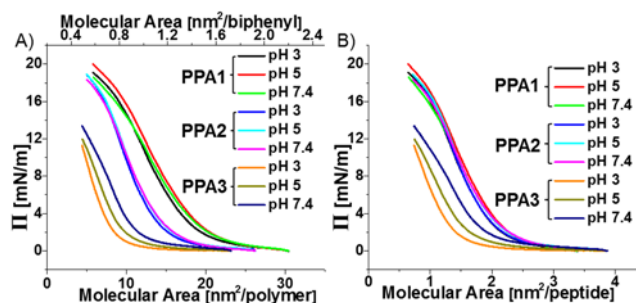


Figure 7. Surface pressure-area isotherms of the PPAs measured on aqueous PBS solutions at 25 °C with varying pH. Molecular area was scaled to the number of (A) polymer molecules along with the number of (A) biphenyl and (B) peptide groups within the PPA. (Could the font be made slightly larger in the plots and then have them side by side instead of stacked? This would save some space, but also look neater and match font sizes in other graphics).

We formed LC-in-PBS emulsions at pH 7.4 with PPAs dissolved in 5CB at concentrations of 1 to 100 mg PPA/mL 5CB. Electrophoretic mobility measurements revealed microdroplets of pure 5CB in PBS to possess a negative ζ -potential of -28 ± 3 mV (Table 1), similar to previous studies showing that hydrophobic surfaces acquire excess negative surface charge density in aqueous

solutions. By contrast, 5CB microdroplets doped with 10 mg/ml PPA1, PPA2 or PPA3 exhibited either positive (30 ± 3 mV), neutral (-5 ± 1 mV) or negative (-55 ± 4 mV) values of ζ -potentials, respectively (Table 1). The PPA-dependent ζ -potentials are consistent with the influence of quaternary ammonium, amide and carboxylic acid groups of PPA1, PPA2 and PPA3, respectively, on the interfacial charging of the LC microdroplets (Figure 6), and thus provide evidence that the PPAs added to the 5CB spontaneously assemble at the aqueous interface of the LC droplets. Furthermore, for all PPAs, the ζ -potential changed significantly when PPA concentration increased from 1 to 10 mg PPA/mL 5CB but remained constant when the PPA concentration increased from 10 to 100 mg PPA/mL 5CB. These results indicate that 10 mg PPA/mL in 5CB corresponds to saturation coverage. We also calculated the ζ -potentials for PPA1 and PPA3-coated 5CB droplets (doped at 10 mg PPA/mL 5CB, Table 1) to correspond to surface charge densities of 0.18 e/nm² and -0.38 e/nm² respectively. The corresponding molecular areas of PPA1 and PPA3 obtained from Figure 5B are ~ 2.4 and ~ 2 nm²/peptide, respectively, consistent with each peptide group at the interface bringing approximately one charge to the interface. Finally, we note that acidification substantially changed the ζ -potentials of the LC droplets decorated with PPA3 but not PPA1 nor PPA2 (Table 2), consistent with our measurements of Π -A isotherms as a function of pH (Figure 5). Based on past studies, the charge status of polymers regulates the organization of polymer interfacial assemblies culminating in LC ordering changes. Therefore, we hypothesized that the transformation of PPA1 or PPA2 to generate structures analogous to PPA3 would lead to changes in polymer-surfactant complexation at the interface of the LCs and thus changes in the ordering of the LCs.

To characterize the influence of interfacial PPAs and PPA-surfactant complexes on the internal ordering of the LC microdroplets (doped with 10 mg PPA/mL 5CB), we used polarized light microscopy (Figure 8). We measured the PPA-decorated LC droplets to exhibit optical signatures characteristic of a so-called bipolar configuration of the LC, which results from LC anchored parallel to the PPA-decorated droplet interface (Figure 8C). However, in contrast to the PPAs, past studies have shown that a range of surfactants with

Table 1. ζ -potentials (mV) of PPA-laden 5CB droplets at various PPA concentrations, measured in PBS at pH 7.4.

	1 mg PPA/ mL 5CB	10 mg PPA/ mL 5CB	100mg PPA/ mL 5CB
PPA1	1 ± 3	30 ± 3	28 ± 2
PPA2	-10 ± 2	-5 ± 1	-5 ± 1
PPA3	-48 ± 3	-55 ± 4	-55 ± 3

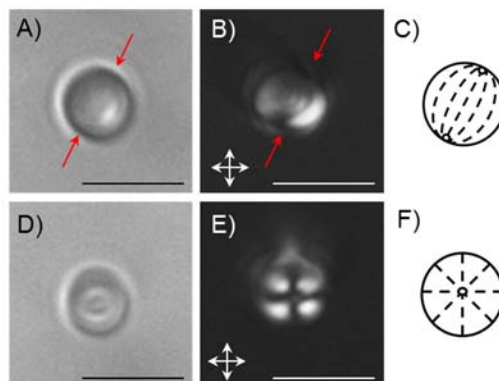


Figure 8. Representative optical micrographs of PPA3-decorated LC microdroplets in the presence of SDS at (A-B) pH 3 and (D-E) 7.4. A and D are bright field images while B and E were obtained using crossed-polars. C and F are schematic illustrations of the ordering of the LC within the microdroplets. Red arrows indicate boojums at the LC microdroplet/aqueous interface. Scale bars are 5 μ m.

linear aliphatic tails, such as sodium dodecylsulfate (SDS) and dodecyltrimethylammonium bromide (DTAB), cause perpendicular orientations of LCs at aqueous interfaces when present at sufficient interfacial concentrations via interdigitation of the surfactant tails with the LC. For microdroplets, the perpendicular orientation of the LC leads to a so-called radial configuration of the microdroplets (Figure 8F). However, surfactants with branched tails, such as Triton X-100, do not perturb the LC from bipolar configurations observed in the absence of adsorbed amphiphile (Figure 8C). To explore the influence of interfacial PPA-surfactant complexes on LC ordering transitions, we next screened PPA-decorated LC microdroplets against solutions of surfactants (triton X-100, DTAB and SDS), using 1 mM surfactant added to the aqueous phase after formation of the PPA-laden 5CB droplets. At pH 7.4, we observed PPA-coated 5CB droplets with or without Triton X-100 to exhibit bipolar configurations. By contrast, exposure to DTAB at pH 7.4 caused radial configurations for bare LC droplets and bipolar configurations when DTAB complexed with PPA interfacial assemblies, indicating that the PPAs changed the interaction between DTAB and the 5CB. SDS at pH 7.4 triggered formation of radial droplets for bare and PPA-laden 5CB droplets (Figure 8D-F), indicating that SDS can complex with the interfacial PPA layer such that interdigitation with 5CB is preserved.

Having observed that Π -A isotherms and ζ -potential measurements revealed that PPA3 but not PPA1 nor PPA2 exhibit pH-dependent interfacial activity, we explored the effect of changes in pH on the PPA-mediated interactions of SDS with the LC microdroplets. Significantly, at pH 3, radial configurations were observed for 5CB droplets decorated with PPA1 and PPA2 while bipolar droplets were found for PPA3-laden 5CB droplets (Figure 3A-C). We note that the carboxylic acid groups of PPA3 are expected to have a pK_a between 2 (pK_a of glycine carboxylic acid) and 5 (pK_a of acetic acid), leading us to conclude that protonation of the carboxylates of PPA3 at pH 3 leads to an interfacial PPA3-SDS complex that prevents the interdigitation of SDS with 5CB.

The results above demonstrate that PPA1 and PPA2 modulate the interaction of SDS with the LC microdroplets at pH 3 in a manner that is distinct from PPA3. We sought to determine if the differential effect of PPA3 relative to PPA1 and PPA2 occurred via differences in either (i) the extent of adsorption of SDS with the PPA-decorated microdroplet or (ii) the organization of co-assemblies formed by PPA and SDS at the LC interface. To achieve this, we performed electrophoretic mobility measurements at pH 3 and 7.4 using PPA-decorated LC microdroplets with and without SDS (Table 2). Significantly, at pH 3, the ζ -potentials of all PPA-decorated 5CB droplets became more negative upon exposure to SDS (Table 2), consistent with SDS adsorption onto the microdroplet interface. This result thus supports our hypothesis that the PPAs mediate the surfactant-triggered response of the LCs not through changes in the extent of adsorption but rather change in the organization of PPA interfacial assemblies and SDS at the interface.

Table 2. ζ -potentials (mV) of bare and PPA-laden 5CB droplets doped at 10 mg PPA/mL 5CB, measured in PBS at different pH conditions with and without SDS present at 1 mM.

	pH 7.4	pH 7.4 w/ SDS	pH 3	pH 3 w/ SDS
5CB	-28 ± 3	-70 ± 5	-7 ± 2	-73 ± 5
PPA1	30 ± 3	-48 ± 2	28 ± 2	-47 ± 2
PPA2	-5 ± 1	-35 ± 2	-5 ± 1	-32 ± 2
PPA3	-55 ± 4	-50 ± 4	-6 ± 2	-38 ± 2

A key result, described above, was identification of experimental conditions under which SDS can be used to develop a differential LC response to PPA3 (the analogue of an enzymatically cleaved PPA1 or PPA2) relative to PPA1 and PPA2. To further evaluate this finding as the basis of a modular and general strategy for triggering LC ordering transitions using biomolecular events, we next characterized the response of LC microdroplets to *in situ* enzymatic treatment of PPA1 and PPA2 decorated 5CB droplets. We formed PPA-containing 5CB aqueous emulsions at pH 7.4 and then incubated the LC droplets with thermolysin. After incubation, the continuous aqueous phase of the emulsion was “developed” using acidified SDS aqueous solutions (Figure 7). Initially, LC droplets decorated with PPA1 and PPA2 exhibited radial configurations after acidified SDS development (0 hr, Figure 7). However, upon incubation with thermolysin, the fraction of LC droplets exhibiting radial configurations decreased with increasing time of thermolysin incubation. Specifically, we observed the optical response of the LC microdroplets to correlate closely with the extent of conversion of the PPA as determined by HPLC (Figure 9). We note that the presence of thermolysin alone does not induce LC ordering transitions in PPA-free LC droplets and thermolysin alone does not prevent SDS interdigitation with LC mesogens at the interface of PPA-free LC droplets. These results demonstrate that SDS can be used to develop the optical response of the LC to enzymatically triggered processing of PPAs.

Overall, these initial experiments demonstrate the design of biologically active PPAs with oligopeptide and biphenyl side-chains that spontaneously assemble at the aqueous interface of LC microdroplets. PPAs can be enzymatically processed to regulate the formation of PPA-surfactant complexes at the LC microdroplet aqueous interface, thus triggering changes in the optical properties of the microdroplets. A significant merit of the approach is that the design of the system is modular, involving specification of (i) the LC-directing functional side-chain of the PPA, (ii) the biologically active oligopeptide of the PPA, and (iii) the synthetic surfactants that differentially interact with the PPA before and after enzymatic processing. This modularity offers the promise of a generalizable approach that makes possible the triggering of LC microdroplet optical properties by a wide range of biomolecular transformations. When combined with recently developed high throughput (10,000 droplets per second) flow-based methods of optically transducing LC microdroplets, such a capability would form the basis of a broadly useful new class of stimuli-responsive supramolecular systems, such as programmable emulsions, and droplet-based microreactor or microanalytical systems.

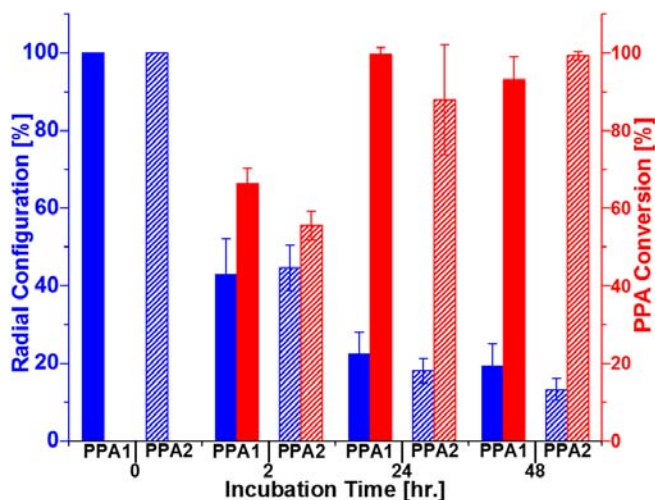


Figure 9. Optical response of LC microdroplets triggered by enzymatic processing of either PPA1 or PPA2, as a function of time of incubation against thermolysin (left axis, blue bars). Extent of PPA conversion, as determined by HPLC (right axis, red bars). Error bars represent triplicates with > 400 droplets analyzed by polarized light microscopy.

Partitioning of Amphiphiles into LCs.

A final advance that we achieved over the grant period involved experiments that were performed to investigate the transport of amphiphiles into and across films of LCs. These experiments were based on 20 μm -thick planar films of nematic 5CB supported on bare glass slides. Initially, we submerged the supported film of LC into pure water. Figure 10A and B show a polarized light micrograph and schematic illustration of the initial state of the system, respectively. The zenithal alignment of the LC (preferred orientation of the LC out of the plane of an interface) at both the aqueous—LC and glass—LC interfaces was determined to be tangential, whereas the azimuthal orientation of the LC (preferred orientation of the LC in the plane of an interface) at both interfaces was degenerate. This director profile within the film resulted in the bright optical appearance of the film shown in Figure 10A.

Previously, we have shown that the cationic surfactant dodecyltrimethylammonium bromide (DTAB) can trigger a transition in the surface ordering of LCs from tangential (planar) to perpendicular (homeotropic) through adsorption at the aqueous—LC interfaces. Thus, we added a concentrated DTAB solution to the aqueous phase above the LC film. The final concentration of DTAB was 2 mM. Interestingly, within 10 minutes after addition of DTAB, the optical appearance remained bright (Figure 10C), and no measurable change in optical retardance of the film was detected (not shown in this report). These results indicate that the LC at both the aqueous—LC and glass—LC interfaces remained in a planar alignment (shown in Figure 10D). We comment here that saturation of the aqueous—LC interface by DTAB should be very fast (within a few seconds). Therefore, we propose that the DTAB monolayer at the aqueous—LC interface leads to a surface anchoring strength that is too weak to induce the elastic strain in the film of the LC that is required to rotate the director at the surface to a perpendicular orientation.

Surprisingly, however, 10 minutes after addition of DTAB, the LC film exhibited a dark optical appearance, indicating a uniform homeotropic alignment of the LC through the film, as shown in Figure 10E. We hypothesize that the homeotropic alignment of the LC at the LC—glass interface was induced by transport of DTAB across the film, and subsequent adsorption of the cationic surfactant to the negatively charged glass slide supporting the film, as shown in Figure 10F. Importantly, these preliminary experimental results suggest that cationic surfactants are able to

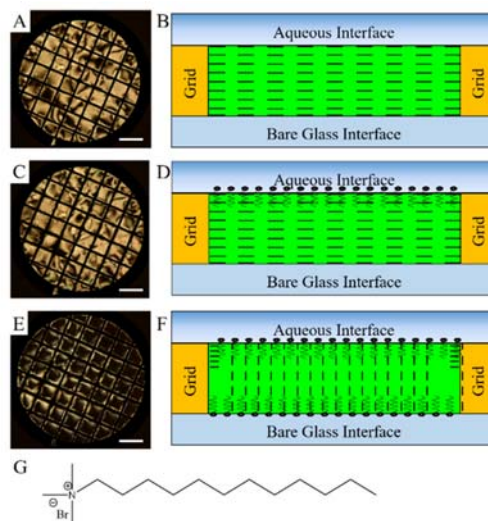


Figure 10. (A, C, E) Polarized light micrographs of a 20 μm -thick film of nematic 5CB submerged in water (A) before, (C) 1 minute and (E) 10 minutes after addition of cationic surfactant DTAB to the aqueous phase above the LC film. (B, D, F) Schematic illustrations of the ordering of the LC within the films shown in (A, C, E), respectively. The concentration of DTAB in C and E is 2 mM. (G) Molecular structure of DTAB.

diffuse across the film of the LCs, and the natural negative charge of the glass provides an electrostatic driving force for the adsorption of the cationic surfactant to the surface of the slide. The findings in this study also suggest that the presence of DTAB at the aqueous—LC interface causes very weak anchoring, in contrast to the mechanism reported in previous studies (DTAB changes the surface ordering of the LC). Future efforts will focus on the influence of the molecular architecture of the amphiphiles and the thickness of the LC film on the temporal evolution of the optical appearance of the LC films.